



Published in final edited form as:

*Neurobiol Dis.* 2020 November ; 145: 105072. doi:10.1016/j.nbd.2020.105072.

## The effect of amyloid on microglia-neuron interactions before plaque onset occurs independently of TREM2 in a mouse model of Alzheimer's disease

Victoria E. von Saucken<sup>a,b</sup>, Taylor R. Jay<sup>b</sup>, Gary E. Landreth<sup>a,b,\*</sup>

<sup>a</sup>Stark Neurosciences Research Institute, Indiana University School of Medicine, Indianapolis, IN 46202, USA

<sup>b</sup>Department of Neurosciences, Case Western Reserve University, Cleveland, OH 44106, USA

### Abstract

Genetic studies identified mutations in several immune-related genes that confer increased risk for developing Alzheimer's disease (AD), suggesting a key role for microglia in AD pathology. Microglia are recruited to and actively modulate the local toxicity of amyloid plaques in models of AD through these cells' transcriptional and functional reprogramming to a disease-associated phenotype. However, it remains unknown whether microglia actively respond to amyloid accumulation before plaque deposition in AD. We compared microglial interactions with neurons that exhibit amyloid accumulation to those that do not in 1-month-old 5XFAD mice to determine which aspects of microglial morphology and function are altered by early 6E10+ amyloid accumulation. We provide evidence of preferential microglial process engagement of amyloid laden neurons. Microglia, on exposure to amyloid, also increase their internalization of neurites even before plaque onset. Unexpectedly, we found that triggering receptor expressed on myeloid cells 2 (TREM2), which is critical for microglial responses to amyloid plaque pathology later in disease, is not required for enhanced microglial interactions with neurons or neurite internalization early in disease. However, TREM2 was still required for early morphological changes exhibited by microglia. These data demonstrate that microglia sense and respond to amyloid accumulation before plaques form using a distinct mechanism from the TREM2-dependent pathway required later in disease.

### Keywords

Amyloid accumulation; Phagocytosis; Neurites; Triggering receptor expressed on myeloid cells 2; Pre-plaque

---

This is an open access article under the CC BY-NC-ND license (<http://creativecommons.org/licenses/by-nc-nd/4.0/>).

\*Corresponding author at: Stark Neurosciences Research Institute, Indiana University School of Medicine, 320 W. 15th St, Indianapolis, IN 46202, USA., [glandret@iu.edu](mailto:glandret@iu.edu) (G.E. Landreth).

Supplementary data to this article can be found online at <https://doi.org/10.1016/j.nbd.2020.105072>.

## 1. Introduction

One of the principal drivers of Alzheimer's disease (AD) is a disruption in amyloid homeostasis, but the response of immune cells to amyloid clearly also plays a key role in AD development and progression (Henstridge et al., 2019). Microglia are brain-resident immune cells that survey the environment through dynamic process extension and retraction (Davalos et al., 2005) and play important roles in normal brain function, including pruning synaptic elements (Weinhard et al., 2018) and clearing apoptotic cells in neurogenic niches (Sierra et al., 2010). In the presence of aberrant activity or damage, microglia rapidly respond by migrating to and extending their processes to affected sites (Davalos et al., 2005; Eyo et al., 2018). This also occurs in AD where microglia cluster at amyloid plaques, changing their morphology, proliferative capacity, and phenotype (Fueger et al., 2017; Meyer-Luehmann et al., 2008). These plaque-associated microglia engage in functions that serve to modulate disease progression, including phagocytosis-mediated clearance of amyloid and apoptotic cells associated with plaques (Fu et al., 2014), and physically restricting plaque growth and diffusion of neurotoxic amyloid species, thereby protecting nearby neurons (Condello et al., 2015; Yuan et al., 2016). However, microglia can also damage surrounding tissue through the production of inflammatory mediators, which can contribute to neuronal dysfunction and cell loss (Hansen et al., 2018; Spangenberg et al., 2016).

It is difficult to determine at late stages of AD what drives these changes in microglial function due to the constellation of pathologic events that occur alongside plaque formation, including neuritic dystrophy, cell death, astrogliosis, and possible infiltration of peripheral immune cells into the brain (Van Eldik et al., 2016). Several studies suggest that microglia sense amyloid accumulation before plaques develop in AD. There is an increase in microglial area in regions with amyloid laden neurons before plaques form in a rat model of AD, and microglia are known to closely associate with neurons at this early stage of disease (Ferretti et al., 2012; Welikovitch et al., 2020; Wilson et al., 2018). It is known that microglia engage in synaptic engulfment before plaque onset (Hong et al., 2016), suggesting that microglia do participate in functionally important interactions with neurons earlier in disease than previously appreciated, but the nature of these early interactions is only beginning to be explored. A recent study showed by laser-capture microdissection of hippocampal neurons in a pre-plaque AD rat model that these amyloid laden cells upregulate the chemokines CCL2 and CCL3, which could serve as cues to recruit microglia to neurons in early disease (Welikovitch et al., 2020). However, it has not been investigated whether microglia preferentially interact with amyloid laden neurons, indicative of their ability to recognize and respond to these cues. Later in disease, microglia phagocytose neurites and neurons, but the extent to which microglia initiate phagocytosis of these substrates prior to plaque accumulation and whether this phagocytic activity is directed specifically toward amyloid laden neurons remain open questions. Furthermore, it remains to be explored whether the mechanisms that orchestrate these early microglial responses in AD differ from those pathways responsible for microglial responses to advanced AD pathologies.

Recent human genetic studies definitively demonstrated that microglia can actively regulate AD pathogenesis. Variants in several immune-related genes confer AD risk (reviewed in Karch and Goate, 2015). Of the immune genes identified, variants of *triggering*

*receptor expressed on myeloid cells 2 (TREM2)* confer the highest risk for developing AD (Guerreiro et al., 2013; Jonsson et al., 2013) and are associated with several other neurodegenerative diseases (Paloneva et al., 2002; Rayaprolu et al., 2013). TREM2 is a single pass transmembrane protein with an IgG-like extracellular domain that signals through DNAX activation protein of 12 kDa (DAP12) to regulate microglial proliferation, survival, migration, phagocytosis, and production of inflammatory factors (Jay et al., 2017b). TREM2 deficiency results in dramatically reduced microglial clustering at amyloid plaques in AD mouse models (Jay et al., 2015; Ulrich et al., 2014; Wang et al., 2015; Yuan et al., 2016) and in individuals with AD (Yuan et al., 2016). In AD mouse models, loss of TREM2 leads to exacerbated amyloid burden at late but not early stages of disease (Jay et al., 2017a) and enhances plaque-associated neuritic dystrophy (Cheng-Hathaway et al., 2018; Wang et al., 2016; Yuan et al., 2016) and neuron loss (Wang et al., 2015). TREM2-deficient microglia also exhibit lower expression of inflammatory and phagocytosis-related genes, suggesting an impairment in these cells' ability to sense or respond to amyloid pathology (Jay et al., 2017a; Jay et al., 2015; Keren-Shaul et al., 2017; Wang et al., 2015). This altogether shows that TREM2 is required for microglial recruitment and responses to amyloid plaques and in doing so, alters AD pathology.

In this study, we find that, before plaque onset in 5XFAD mice, microglia preferentially orient their processes toward amyloid laden neurons and increase their coverage of brain regions with high levels of amyloid accumulation. These microglia also display morphological changes and exhibit enhanced phagocytic activity. We show that the loss of the microglial receptor TREM2 impairs amyloid-driven shifts in microglial morphology, but interestingly, does not affect microglia-neuron interactions nor microglial phagocytic activity at this early stage of disease. These data reveal that the mechanisms controlling these microglial functions later in disease are distinct from those mediating the same functional changes before plaque onset.

## 2. Materials and methods

### 2.1. Animals

5XFAD transgenic mice (APP<sup>SwF1L</sup>on, PSEN1<sup>\*M146L\*L286V</sup>) from Jackson Laboratory overexpressing mutant forms of human APP and PSEN1 under the mouse *Thy1* promoter (Oakley et al., 2006) were used at 1 month of age to model early amyloid pathology in AD. To generate 5XFAD; *Trem2*<sup>-/-</sup> mice, we crossed 5XFAD mice to *Trem2*<sup>-/-</sup> mice (TREM2<sup>tm1(KOMP)Vl</sup>cg), which substitutes a lacZ reporter for exons 2, 3 and a part of exon 4 of *Trem2* (Jay et al., 2015). This mouse model has previously been shown to also exhibit specific misregulation of the neighboring gene *Trem1* (Kang et al., 2018), though studies so far have found that this model largely recapitulates other TREM2 KO models in studies of AD (Cheng-Hathaway et al., 2018; Jay et al., 2017a). Littermate controls and both sexes were used in all experiments for a total of  $n = 8$  5XFAD mice (6 males, 2 females) and  $n = 9$  5XFAD; *Trem2*<sup>-/-</sup> mice (5 males, 4 females), except neurite contact and internalization analyses where a randomized sample of  $n = 6$  5XFAD; *Trem2*<sup>-/-</sup> mice were used. All mice were maintained on a C57BL/6 J background. Data were collected from mice housed in the animal facilities at Case Western Reserve University and at Stark

Neurosciences Research Institute at Indiana University School of Medicine. The results were similar in animals from both institutes. Our protocol was approved by the Case Western Reserve University and the Indiana University School of Medicine IACUC committees. All mice had ad libitum access to food and water and were maintained on a 12 h light-dark cycle.

## 2.2. Slice preparation and Immunofluorescence

Mice were perfused with PBS and one brain hemisphere drop fixed in 4% PFA in PBS at 4 °C overnight and stored in 30% sucrose in PBS at 4 °C. Brains were embedded in O.C.T Compound (VWR) and cryosectioned into 30 µm free floating sections that were stored in cryoprotectant buffer at -20 °C until further use. Brain slices were permeabilized in PBS with 0.1% Triton-X and antigen retrieval was conducted at 85 °C for 15 min and then cooled at room temperature for 30 min using 10 mM sodium citrate with 0.5% Tween pH 6.0, except when staining for MAP2 and phosphorylated-neurofilament (pNF), where Reveal Decloaker (Biocare Medical, RV1000) was used. Slices were blocked (5% normal goat or donkey serum, 0.3% Triton-X in PBS pH 7.4) for 1 h and incubated in the following primary antibodies overnight at 4 °C: beta-amyloid 1-16 6E10 (Biolegend 803001, 1:1000), Iba1 (Wako 019-19741, 1:1000-1:2000), MAP2 (Abcam ab5392, 1:2000), NeuN (Millipore ABN90P, 1:1500), and pNF (Biolegend 801601, 1:1000). Slices were washed, and incubated with Alexa-fluor conjugated secondary antibodies at a 1:1000 dilution for 1 h at room temperature. Slices were stained with a 1:10000 dilution of DAPI in PBS, washed and mounted using Prolong Gold.

## 2.3. Image acquisition and analysis

For each experiment, staining was performed on 1 medial and 1 lateral sagittal brain section per animal, and the investigator was blinded to *Trem2* genotype. All images were acquired on the Nikon confocal microscope with optical slices set at 0.775 µm across 30 µm sections with a 40× oil objective (NA = 1.3), except for microglia-neurite contact and internalization imaging which was done with a 60× oil objective (NA = 1.4).

## 2.4. Microglial number, coverage, and neuron engagement

Brain sections were stained for Iba1, NeuN, and 6E10. Two brain sections were analyzed for each animal. For each brain section, two regions of interest (ROIs) with high amyloid levels in the somatosensory cortex and one ROI with low amyloid levels in the visual cortex were imaged for a total of four images in the somatosensory cortex and two images in the visual cortex per animal. Images were thresholded and maximum projections were prepared from z-stacks. NeuN was used to define cortical layer V for each image and within this area, the number of Iba1+ cells were manually counted and percent Iba1+ area was measured using Image J. These values were then averaged across all images acquired for each brain region in each animal, and statistics and graphs represent these averaged values. To assess microglial engagement of neurons, a circle was drawn centered on each neuronal cell body with a 25 µm diameter. Since each of the neurons examined here had a diameter of approximately 20 µm, this represented a distance of roughly 2.5 µm surrounding each cell body. A blinded observer then used this to establish the number of microglial processes that were in close proximity to the neuronal cell body. This heuristic was then applied to neurons across the

field of view for each image. For each animal, two ROIs were imaged in the somatosensory cortex, with a total of 89 to 104 NeuN+ cells analyzed per animal. These cells were divided into 6E10+ and 6E10- cell subsets based on the presence of 6E10 signal with a total of 37 to 52 cells in each group for each animal. The average number of Iba1+ processes in close proximity with NeuN+ cell bodies was reported as microglial interaction or engagement of neurons. Using 3D z-stacks on Image J, the number of NeuN+ cells with soma-soma contact from an Iba1+ cell was manually counted in these same fields (89 to 104 cells over 2 ROIs in the somatosensory cortex per animal). Analyses for these microglial interaction measures were performed on cellular replicates from 5XFAD *Trem2*<sup>+/+</sup> animals for a total of 416 6E10+ cells and 401 6E10- cells. These analyses were also included in supplemental material on cellular replicates from 5XFAD *Trem2*<sup>-/-</sup> (KO) animals for a total of 468 6E10+ cells and 453 6E10- cells.

## 2.5. Microglial morphology

Sholl analysis adapted from Norris et al. (2014) was performed to evaluate microglial morphology. Brain sections were stained for Iba1 and images were acquired, thresholded, and maximum projections were prepared from z-stacks. All cells completely encompassed within each ROI that could be clearly distinguished from neighboring cells were analyzed. Between 5 and 7 cells met these criteria per ROI, and a minimum of 10 cells over two ROIs within the somatosensory cortex and visual cortex were analyzed per animal. The length of the longest process was determined manually by drawing a line from the center of the cell body to the tip of the most distal process and the length recorded using Image J. To determine the total number of intersections, concentric radii were established 5  $\mu\text{m}$  apart starting at 1  $\mu\text{m}$  from the edge of the cell body, continuing to the most distal process. The number of microglial branches that intersected with all radii was recorded using the Sholl analysis plugin in Image J. Analysis was performed on cellular replicates, as previously described (Norris et al., 2014).

## 2.6. Microglial contact and internalization of neurites

Immunofluorescence was conducted for Iba1, pNF, and MAP2, and 60 $\times$  confocal images were acquired. DAPI was used to locate cortical layer V. Images were deconvoluted in 3D, thresholded, and binary layers applied for Iba1, pNF, and MAP2 to create 3D reconstructed images using NIS Software (Nikon). With these binary images, the number of pNF+ or MAP2+ objects within 2  $\mu\text{m}^3$  of an Iba1+ cell were counted in an automated fashion using the NIS General Analysis 3D program. These results were reported as the percentage of engaged neurites from total neurites, averaged across the 3D fields of two ROIs per cortical area for each animal. Microglial internalization of neurites was determined by measuring the volume of neuritic components specifically within Iba1+ cell volume (referred to as internalized neurites) and the total volume of neuritic components within the 3D field to calculate the percentage of internalized neurites within microglia. This was done individually for MAP2+ dendrites and pNF+ axons in, as above, two ROIs for each cortical region in each animal. It should be noted that z slices were acquired 0.775  $\mu\text{m}$  apart. While this is consistent with previous work that performed similar analyses (Sierra et al., 2010), oversampling in the z plane using smaller step sizes would have allowed us to better ensure that all the co-localized signal we observed was truly represented co-localized in the

z plane. The pNF+ and MAP2+ signal within Iba1+ cells reported here was determined in an automated fashion using 3D co-localization analysis in Nikon NIS software.

## 2.7. Statistics

Statistical analyses were performed using GraphPad Prism. Statistical differences across two groups were determined using two-sided, unpaired *t*-tests on individual cells (NeuN+ or Iba1+ cells) and two-sided, paired *t*-tests performed for analyses that assessed differences across brain regions within animals, as denoted in each figure legend. 2-way ANOVAs were used in comparisons of amyloid level and *Trem2* genotype and Bonferroni post-hoc tests performed where indicated. Column statistics were applied to identify outliers and these samples were excluded. Each *n* represents an individual animal, except for assessment of microglial morphology and microglial engagement of cell bodies where cellular replicates were used for analysis. Graphs represent the mean and error bars signify the SEM.

Significance between groups are denoted by \*  $p < 0.05$ , \*\*  $p < 0.01$ , \*\*\*  $p < 0.001$ , or \*\*\*\*  $p < 0.0001$ . In addition, means, SEM, *n*'s and exact *p*-values are included in the figure legend for each analysis.

## 3. Results

### 3.1. Early neuron-associated amyloid accumulation in an AD mouse model

To address how microglia respond to amyloid pathology before plaque onset, we examined 1-month-old 5XFAD mice. In this AD model, plaques have not yet formed at 1 month of age, but 6E10 immunoreactive species are found to accumulate within neurons (Fig. 1A), including amyloid precursor protein and its amyloidogenic cleavage products (Youmans et al., 2012).

### 3.2. Microglial coverage and morphology in high and low amyloid laden brain areas

Because there are regional differences in the accumulation of 6E10+ amyloid species in our model, we were able to compare areas of low amyloid accumulation (visual cortex, Fig. 1B) to those with high levels (somatosensory cortex, Fig. 1C). We were interested in what early changes occur in microglia in response to amyloid accumulation and evaluated microglia number, coverage, and morphology in the visual (Fig. 1D–E) and somatosensory cortices (Fig. 1F–G). We found an increase in Iba1+ microglial area within cortical regions with high amyloid levels compared to low levels (Fig. 1H), indicating that even in the absence of plaques, amyloid can drive enhanced area coverage by microglia.

Both changes in the number of microglia or their morphology could promote increased microglial area in amyloid laden brain regions, and both of these features of microglia are established to change after the onset of plaque deposition. At this early stage of disease, we found no change in the number of microglia in areas with high amyloid levels (Fig. 1I) and no change in the length of the longest process of individual microglia (Fig. 1J). However, Sholl analysis revealed an increase in the number of intersections between microglial processes and concentric radii established around the cell body, a measure used to determine microglial branching complexity, within high amyloid regions (Fig. 1K). These early morphological changes thus contribute to the increases in microglial coverage of areas

with high amyloid levels early in pathology. Interestingly, this is in contrast to the reduced branching observed in activated microglia after plaque onset, indicating that microglia exhibit distinct morphological changes at early and late stages of AD.

### 3.3. Microglial engagement of neurons

These data suggest that microglia respond to early amyloid accumulation before plaque onset through morphological changes. However, these comparisons were done across different cortical areas and intrinsic differences in microglia between these two regions could also contribute to these results. To determine whether our results were due specifically to microglial sensing early amyloid accumulation, we next evaluated microglial responses within the somatosensory cortex, which contains both neurons that do and do not exhibit early amyloid accumulation based on positive 6E10 signal at this stage of disease. We used this region to assess whether microglia preferentially associated with amyloid laden neurons. It is well described that plaques readily recruit microglia and that plaque-associated microglia preferentially orient their processes to contact plaques (Meyer-Luehmann et al., 2008). We found that early amyloid build-up also elicits preferential microglial association with 6E10+ neurons (Fig. 2A), similar to previous reports (Ferretti et al., 2012; Wilson et al., 2018). Next we quantified these microglia-neuron interactions and observed an increase in the number of microglial processes adjacent to or contacting 6E10+ neuronal cell bodies compared to neighboring neurons lacking 6E10 signal in the somatosensory cortex (Fig. 2B). We next compared the distribution of microglial contacts on neuronal cell bodies between 6E10+ and 6E10- neuronal populations. We observed a greater number of 6E10- neurons with no or minimal microglial contacts (0 to 2 engaged processes) compared to 6E10+ neurons, whereas significantly more 6E10+ neurons had 5 or 6 engaged microglial processes relative to 6E10- neurons (Fig. 2C). These findings indicate a shift in microglia-neuron interactions from minimal to extensive microglial process contact of neuronal cell bodies in response to amyloid accumulation. This extends recent work eloquently demonstrating increased microglial process contact of neuronal cell bodies in stroke, suggesting that these interactions may represent a common functional response of microglia to neurons across diverse injury and disease states (Cserép et al., 2020). In addition to microglial processes, microglial cell bodies have also been shown to contact neuronal cell bodies, which had been shown to precede the phagocytic removal of neurons (Sierra et al., 2010). Using NeuN to identify neuronal cell bodies, we observed cell body contacts between microglia and neurons in this early stage of pathology within the somatosensory cortex (Fig. 2D). Similar to microglia process engagement of neuronal cell bodies, these soma-soma interactions were enhanced for 6E10+ neurons compared to neighboring 6E10- neurons (Fig. 2E). Altogether, we show that microglia respond to early amyloid accumulation through process and cell body contact of neurons with a local preference for amyloid laden neurons.

### 3.4. Neurite contacts by microglia

We also observed close interactions between microglial processes and neurites (Fig. 3A–B) in the somatosensory and visual cortices. Previous studies have used varying distances from 13 nm to 50  $\mu$ m as cut-offs to study microglial mobilization and contact of neurons (Cserép et al., 2020; Welikovitch et al., 2020). To assess possible sites of interaction between

microglia and neurites, we quantified the number of neurites within  $2 \mu\text{m}^3$  of a microglial cell, consistent with the distance used to assess microglial interactions with neuronal cell bodies in our previous analyses. Using 3D reconstruction of thresholded, binary-converted confocal images (Fig. 3C,E), we quantified the percentage of pNF+ axons or MAP2+ dendrite objects within  $2 \mu\text{m}^3$  of an Iba1+ microglia relative to total neurites within the field to measure potential microglia-neurite interactions. We found an increase in microglial association with both axons (Fig. 3D) and dendrites (Fig. 3F) in areas with higher amyloid, indicating enhanced local engagement of microglia with neurites in the presence of amyloid accumulation.

### 3.5. Amyloid-induced neurite internalization by microglia

These data demonstrate that microglia recognize and respond to amyloid pathology before plaque onset by changing their morphology and increasing their interaction with neuronal cell bodies and neurites. We next wanted to determine whether these structural interactions also represent important functional interactions between microglia and neurons early in disease. We hypothesized that an amyloid-driven increase in microglia-neuron interactions could correlate with enhanced microglial internalization of neuritic components, thereby contributing to early AD pathology. We observed internalized pNF+ axon fragments within Iba1+ microglia (Fig. 4A), and found a significant effect of brain region on internalized axons and dendrites by microglia (Fig. 4B–C). However, it should be noted that while similar to those used in previous studies (Sierra et al., 2010), the imaging parameters used here do result in undersampling in the z plane, and thus the co-localization may be overestimated. However, these data show that microglial engulfment of neurites occurs relatively more in response to amyloid production, preceding the appearance of plaques in our 5XFAD model. It is known that microglial elimination of synapses, neurites, and neurons that occurs later with disease progression are critical determinants of behavioral changes associated with AD pathology (Shi et al., 2017; Spangenberg et al., 2016). Our data indicate that these amyloid-driven changes in microglial phagocytic function may occur earlier in disease than previously appreciated, initiating early changes in neuronal function that likely have an important impact on later behavioral deficits in AD.

### 3.6. TREM2 is not required for early microglial responses to amyloid accumulation

TREM2 is necessary after plaque development to orchestrate changes in microglial phenotype, accumulation around plaques, and clearance of amyloid species (Jay et al., 2017b; Wang et al., 2016; Yuan et al., 2016). We used 5XFAD TREM2 KO mice to determine whether TREM2 was also required for the changes in microglial function observed at 1 month of age. It should be noted that the TREM2 KO model used here has also been shown to increase transcription of the gene *Trem1* (Kang et al., 2018). Using this model, we found that TREM2 was required for the morphological changes in microglia in response to early amyloid accumulation (Fig. S1). However, TREM2 was not required for preferential recruitment of microglial processes to amyloid laden neurons (Fig. S2) or for uptake of neurites (Fig. 4B,C). This differs from the clear role of TREM2 in microglial recruitment to amyloid plaques. These findings overall show that early structural and functional changes in microglia-neuron interactions do not require TREM2, and must

rely on mechanisms distinct from those that drive microglial responses to amyloid plaques and phagocytosis later in disease.

#### 4. Discussion

In this study we provide novel insights into the phenotypic changes that microglia undergo in early AD before plaque onset and address how the mechanisms that govern these changes compare to those required for microglial responses to AD pathology after plaque deposition. We used the region-specific and relatively sparse amyloid accumulation within neurons in 1-month-old 5XFAD mice to assess whether microglial phenotype was specifically altered in response to neuronal amyloid accumulation. Indeed, we found that there was an increase in the area occupied by microglia in regions with extensive neuronal amyloid accumulation. TREM2 is known to be required for microglial chemotaxis (Mazaheri et al., 2017) and clustering in areas with high levels of amyloid after plaque deposition (Jay et al., 2017a; Wang et al., 2015). To assess whether the same mechanism was responsible for changes in microglial morphology and coverage before plaque onset, we tested whether these changes were also dependent on TREM2. Our study reveals that TREM2 is required to initiate changes in microglial morphology and increased microglial coverage of amyloid laden cortical areas before plaques form. This demonstrates that microglial accumulation and morphological changes share a TREM2-dependent mechanism throughout AD progression.

We show, for the first time, that microglia in regions with neuronal amyloid accumulation preferentially engage with these amyloid laden neurons, supporting neuronal amyloid accumulation as a driver of microglial engagement. We find that microglia engage in a range of interactions with neurons in early AD, including process-soma, soma-soma, and process-neurite contacts. It has been posited that TREM2 is required to sense amyloid deposition later in AD progression (Zhao et al., 2018). We found that before plaques deposit, TREM2 deficient microglia displayed no differences in their ability to preferentially engage 6E10+ neurons, suggesting that TREM2 is not required for microglial responses to neuronal amyloid accumulation in early AD. We were not able to identify the factors that are responsible for driving this microglial engagement with neurons early in pathology in this study. Previous work in other pathological contexts suggest candidate factors, including chemokines such as CX3CL1 (Lee et al., 2014) and CCL2/3 (Welikovitch et al., 2020), factors released in response to oxidative stress (Wilson et al., 2018), myelin debris, or extracellular ATP (Cserép et al., 2020; Davalos et al., 2005; Neumann et al., 2009). Factors involved in microglia-neuron interactions during development, including complement or phosphatidylserine (PS) exposure (Scott-Hewitt et al., 2020) could also play a role in the interactions we observe here in early AD. Recently, microglial interactions with neuronal soma have been linked to the level of neuronal activity, supported by TRPV1-expressing neurons activated by capsaicin exhibiting increased soma contacts by microglia (Hughes and Appel, 2020). This brings forth a new dimension to microglia-neuron interactions, neuronal synaptic transmission, which may also be a key regulator of microglial engagement of neurons in early AD. It is not yet clear how intraneuronal amyloid accumulation might interact with these, or yet-to-be identified factors, to promote specific microglial recruitment to 6E10+ neurons. While future work will be required to delineate the specific cues at play, our data demonstrate that early amyloid accumulation is sufficient to promote preferential

engagement of amyloid laden neurons over neighboring neurons by microglia irrespective of TREM2 expression before plaque formation in AD.

In light of recent studies showing that microglial contacts are associated with synapse remodeling (Weinhard et al., 2018) and dendritic spine loss (Tremblay et al., 2010), we posited that the early interactions we observe between microglia and neurons in AD could indicate functional alterations in phagocytic uptake of neuronal elements by microglia early in disease. At late stages of AD, microglia engage in phagocytosis of neurons, contributing to pathological neuronal loss (Spangenberg et al., 2016). However, extensive neuronal cell death is not observed at the early disease stage examined in our study (Oakley et al., 2006), bringing forth the question of what role microglial phagocytosis has early in AD. Rather than executing phagocytosis of neuronal cell bodies, we found that microglia internalize neuritic elements. Microglial engulfment of neurites was enhanced in areas with high levels of amyloid accumulation, signifying that amyloid may direct microglial phagocytic uptake of neurites at this early pathologic stage. Neuritic uptake by microglia may lead to synaptic dysfunction through the active process of synaptic pruning, which has previously been shown to occur at 1 month of age before plaque onset in a mouse model of AD (Hong et al., 2016). The refinement of synaptic connectivity in these brain regions is complete by 1 month of age, however, it would be illuminating to examine these phenomena at later disease stages and in a less aggressive AD model before plaque onset. In our model, TREM2 deficiency did not suppress microglial uptake of neurites, suggesting that different regulatory mechanisms control microglial phagocytic activity at early and late stages of disease since TREM2 is known to coordinate the upregulation of phagocytic machinery late in disease (Keren-Shaul et al., 2017). While some of the microglia-neuron contacts we observed in response to early AD pathology result in phagocytosis, recent work shows that microglia-neuron contacts do not always represent phagocytic interactions, instead serving a protective function following stroke (Cserép et al., 2020). Future work will likely uncover other important functions of these microglia-neuron interactions in disease that may be helpful, harmful, or simply represent passive surveillance.

We find amyloid accumulation preceding plaque onset is sufficient to change microglial morphology and promote microglial process engagement and phagocytic machinery targeting amyloid laden neurons. While normally considered a coordinated response of microglia to disease, our data suggest that amyloid-driven morphological changes are governed by a TREM2-dependent pathway, whereas TREM2-independent pathways are responsible for microglial interactions with neurons and phagocytosis of neurites. This suggests it is possible to manipulate specific features of the microglial response to AD pathology, which may be critically important in the design of microglia-directed AD therapeutics.

## Supplementary Material

Refer to Web version on PubMed Central for supplementary material.

## Acknowledgements

We thank all members of the Landreth, Lamb, and Lasagna-Reeves labs in the Stark Neurosciences Research Institute for thoughtful discussions and technical support. Additionally, we thank Hyejin Kim for perfectly capturing our ideas in the graphical abstract, and Ulf Dettmer for critically reading the manuscript. This work was supported by grants from the National Institute of Health (AG051495 and AG050597 to GEL), NIA National Research Service Award F31 (AG048704 to TRJ), and the Alzheimer's Association (BFG-15-364590 to GEL).

## Abbreviations

<b>AD</b>	Alzheimer's disease
<b>TREM2</b>	Triggering receptor expressed on myeloid cells 2

## References

- Cheng-Hathaway PJ, Reed-Geaghan EG, Jay TR, Casali BT, Bemiller SM, Puntambekar SS, von Saucken VE, Williams RY, Karlo JC, Moutinho M, Xu G, Ransohoff RM, Lamb BT, Landreth GE, 2018. The TREM2 R47H variant confers loss-of-function-like phenotypes in Alzheimer's disease. *Mol. Neurodegener* 13 (1), 29. 10.1186/s13024-018-0262-8. [PubMed: 29859094]
- Condello C, Yuan P, Schain A, Grutzendler J, 2015. Microglia constitute a barrier that prevents neurotoxic protofibrillar A $\beta$ 42 hotspots around plaques. *Nat. Commun* 6, 6176. 10.1038/ncomms7176. [PubMed: 25630253]
- Cseré C, Pósfai B, Lénárt N, Fekete R, László ZI, Lele Z, Orsolits B, Molnár G, Heindl S, Schwarcz AD, Ujvári K, Környei Z, Tóth K, Szabadits E, Sperlágh B, Baranyi M, Csiba L, Hortobágyi T, Maglóczky Z, Martinecz B, Szabó G, Erdélyi F, Szips R, Tamkun MM, Gesierich B, Dering M, Katona I, Liesz A, Tamás G, Dénes A, 2020. Microglia monitor and protect neuronal function through specialized somatic purinergic junctions. *Science* 367 (6477), 528–537. 10.1126/science.aax6752. [PubMed: 31831638]
- Davalos D, Grutzendler J, Yang G, Kim JV, Zuo Y, Jung S, Littman DR, Dustin ML, Gan WB, 2005. ATP mediates rapid microglial response to local brain injury in vivo. *Nat. Neurosci* 8 (6), 752–758. 10.1038/nn1472. [PubMed: 15895084]
- Eyo UB, Bispo A, Liu J, Sabu S, Wu R, DiBona VL, Zheng J, Murugan M, Zhang H, Tang Y, Wu LJ, 2018. The GluN2A subunit regulates neuronal NMDA receptor-induced microglia-neuron physical interactions. *Sci. Rep* 8 (1), 828. 10.1038/s41598-018-19205-4. [PubMed: 29339791]
- Ferretti MT, Bruno MA, Ducatenzeiler A, Klein WL, Cuello AC, 2012. Intracellular A $\beta$ -oligomers and early inflammation in a model of Alzheimer's disease. *Neurobiol. Aging* 33 (7), 1329–1342. 10.1016/j.neurobiolaging.2011.01.007. [PubMed: 21414686]
- Fu R, Shen Q, Xu P, Luo JJ, Tang Y, 2014. Phagocytosis of microglia in the central nervous system diseases. *Mol. Neurobiol* 49 (3), 1422–1434. 10.1007/s12035-013-8620-6. [PubMed: 24395130]
- Fueger P, Hefendehl JK, Veeraghavalu K, Wendeln AC, Schlosser C, Obermueller U, Wegenast-Braun BM, Neher JJ, Martus P, Kohsaka S, Thunemann M, Feil R, Sisodia SS, Skodras A, Jucker M, 2017. Microglia turnover with aging and in an Alzheimer's model via long-term in vivo single-cell imaging. *Nat. Neurosci* 20 (10), 1371–1376. 10.1038/nn.4631. [PubMed: 28846081]
- Guerreiro R, Wojtas A, Bras J, Carrasquillo M, Rogava E, Majounie E, Cruchaga C, Sassi C, Kauwe JS, Younkin S, Hazrati L, Collinge J, Pockock J, Lashley T, Williams J, Lambert JC, Amouyel P, Goate A, Rademakers R, Morgan K, Powell J, St George-Hyslop P, Singleton A, Hardy J, Alzheimer Genetic Analysis Group, 2013. TREM2 variants in Alzheimer's disease. *N. Engl. J. Med* 368 (2), 117–127. 10.1056/NEJMoa1211851. [PubMed: 23150934]
- Hansen DV, Hanson JE, Sheng M, 2018. Microglia in Alzheimer's disease. *J. Cell Biol* 217 (2), 459–472. 10.1083/jcb.201709069. [PubMed: 29196460]
- Henstridge CM, Hyman BT, Spires-Jones TL, 2019. Beyond the neuron-cellular interactions early in Alzheimer disease pathogenesis. *Nat. Rev. Neurosci* 20 (2), 94–108. 10.1038/s41583-018-0113-1. [PubMed: 30643230]

- Hong S, Beja-Glasser VF, Nfonoyim BM, Frouin A, Li S, Ramakrishnan S, Merry KM, Shi Q, Rosenthal A, Barres BA, Lemere CA, Selkoe DJ, Stevens B, 2016. Complement and microglia mediate early synapse loss in Alzheimer mouse models. *Science* 352 (6286), 712–716. 10.1126/science.aad8373. [PubMed: 27033548]
- Hughes AN, Appel B, 2020. Microglia phagocytose myelin sheaths to modify developmental myelination. *Nat. Neurosci* 10.1038/s41593-020-0654-2.
- Jay TR, Miller CM, Cheng PJ, Graham LC, Bemiller S, Broihier ML, Xu G, Margevicius D, Karlo JC, Sousa GL, Cotleur AC, Butovsky O, Bekris L, Staugaitis SM, Leverenz JB, Pimplikar SW, Landreth GE, Howell GR, Ransohoff RM, Lamb BT, 2015. TREM2 deficiency eliminates TREM2+ inflammatory macrophages and ameliorates pathology in Alzheimer's disease mouse models. *J. Exp. Med* 212 (3), 287–295. 10.1084/jem.20142322. [PubMed: 25732305]
- Jay TR, Hirsch AM, Broihier ML, Miller CM, Neilson LE, Ransohoff RM, Lamb BT, Landreth GE, 2017a. Disease progression-dependent effects of TREM2 deficiency in a mouse model of Alzheimer's disease. *J. Neurosci* 37 (3), 637–647. 10.1523/JNEUROSCI.2110-16.2016. [PubMed: 28100745]
- Jay TR, von Saucken VE, Landreth GE, 2017b. TREM2 in neurodegenerative diseases. *Mol. Neurodegener* 12 (1), 56. 10.1186/s13024-017-0197-5. [PubMed: 28768545]
- Jonsson T, Stefansson H, Steinberg S, Jonsdottir I, Jonsson PV, Snaedal J, Bjornsson S, Huttenlocher J, Levey AI, Lah JJ, Rujescu D, Hampel H, Giegling I, Andreassen OA, Engedal K, Ulstein I, Djurovic S, Ibrahim-Verbaas C, Hofman A, Ikram MA, van Duijn CM, Thorsteinsdottir U, Kong A, Stefansson K, 2013. Variant of TREM2 associated with the risk of Alzheimer's disease. *N. Engl. J. Med* 368 (2), 107–116. 10.1056/NEJMoa1211103. [PubMed: 23150908]
- Kang SS, Kurti A, Baker KE, Liu C-C, Colonna M, Ulrich JD, Holtzman DM, Bu G, Fryer JD, 2018. Behavioral and transcriptomic analysis of Trem2-null mice: not all knockout mice are created equal. *Hum. Mol. Genet* 27 (2), 211–223. 10.1093/hmg/ddx366. [PubMed: 29040522]
- Karch CM, Goate AM, 2015. Alzheimer's disease risk genes and mechanisms of disease pathogenesis. *Biol. Psychiatry* 77 (1), 43–51. 10.1016/j.biopsych.2014.05.006. [PubMed: 24951455]
- Keren-Shaul H, Spinrad A, Weiner A, Matcovitch-Natan O, Dvir-Szternfeld R, Ulland TK, David E, Baruch K, Lara-Astaiso D, Toth B, Itzkovitz S, Colonna M, Schwartz M, Amit I, 2017. A unique microglia type associated with restricting development of Alzheimer's disease. *Cell* 169 (7), 1276–1290. 10.1016/j.cell.2017.05.018. [PubMed: 28602351]
- Lee S, Xu G, Jay TR, Bhatta S, Kim K, Jung S, Landreth GE, Ransohoff RM, Lamb BT, 2014. Opposing effects of membrane-anchored CX3CL1 on amyloid and tau pathologies via the p38 MAPK pathway. *J. Neurosci* 34 (37), 12538–12546. 10.1523/JNEUROSCI.0853-14.2014. [PubMed: 25209291]
- Mazaheri F, Snaidero N, Kleinberger G, Madore C, Daria A, Werner G, Krasemann S, Capell A, Truembach D, Wurst W, Brunner B, Bultmann S, Tahirovic S, Kerschensteiner M, Misgeld T, Butovsky O, Haass C, 2017. TREM2 deficiency impairs chemotaxis and microglial responses to neuronal injury. *EMBO Rep* 18 (7), 1186–1198 Doi: 10.15252/embr.201743922. [PubMed: 28483841]
- Meyer-Luehmann M, Spires-Jones TL, Prada C, Garcia-Alloza M, de Calignon A, Rozkalne A, Koenigsknecht-Talboo J, Holtzman DM, Bacskai BJ, Hyman BT, 2008. Rapid appearance and local toxicity of amyloid-beta plaques in a mouse model of Alzheimer's disease. *Nature* 451 (7179), 720–724. 10.1038/nature06616. [PubMed: 18256671]
- Neumann H, Kotter MR, Franklin RJ, 2009. Debris clearance by microglia: an essential link between degeneration and regeneration. *Brain* 132 (Pt 2), 288–295. 10.1093/brain/awn109. [PubMed: 18567623]
- Norris G, Derecki N, Kipnis J, 2014. Microglial Sholl Analysis. Retrieved from. 10.1038/protex.2014.029.
- Oakley H, Cole SL, Logan S, Maus E, Shao P, Craft J, Guillozet-Bongaarts A, Ohno M, Disterhoft J, Van Eldik L, Berry R, Vassar R, 2006. Intraneuronal beta-amyloid aggregates, neurodegeneration, and neuron loss in transgenic mice with five familial Alzheimer's disease mutations: potential factors in amyloid plaque formation. *J. Neurosci* 26 (40), 10129–10140. 10.1523/JNEUROSCI.1202-06.2006. [PubMed: 17021169]

- Paloneva J, Manninen T, Christman G, Hovanes K, Mandelin J, Adolfsson R, Bianchin M, Bird T, Miranda R, Salmaggi A, Tranebjaerg L, Kontinen Y, Peltonen L, 2002. Mutations in two genes encoding different subunits of a receptor signaling complex result in an identical disease phenotype. *Am. J. Hum. Genet* 71 (3), 656–662. 10.1086/342259. [PubMed: 12080485]
- Rayaprolu S, Mullen B, Baker M, Lynch T, Finger E, Seeley WW, Hatanpaa KJ, Lomen-Hoerth C, Kertesz A, Bigio EH, Lippa C, Josephs KA, Knopman DS, White CL 3rd, Caselli R, Mackenzie IR, Miller BL, Boczarska-Jedynak M, Opala G, Krygowska-Wajs A, Barcikowska M, Younkin SG, Petersen RC, Ertekin-Taner N, Uitti RJ, Meschia JF, Boylan KB, Boeve BF, Graff-Radford NR, Wszolek ZK, Dickson DW, Rademakers R, Ross OA, 2013. TREM2 in neurodegeneration: evidence for association of the p.R47H variant with frontotemporal dementia and Parkinson's disease. *Mol Neurodegener* 8, 19. 10.1186/1750-1326-8-19. [PubMed: 23800361]
- Scott-Hewitt N, Perrucci F, Morini R, Erreni M, Mahoney M, Witkowska A, Carey A, Faggiani E, Schuetz LT, Mason S, Tamborini M, Bizzotto M, Passoni L, Filipello F, Jahn R, Stevens B, Matteoli M, 2020. Local externalization of phosphatidylserine mediates developmental synaptic pruning by microglia. *EMBO J* e105380 Doi: 10.15252/embj.2020105380. [PubMed: 32657463]
- Shi Q, Chowdhury S, Ma R, Le KX, Hong S, Caldarone BJ, Stevens B, Lemere CA, 2017. Complement C3 deficiency protects against neurodegeneration in aged plaque-rich APP/PS1 mice. *Sci Transl Med* 9 (392). 10.1126/scitranslmed.aaf6295.eaaf6295.
- Sierra A, Encinas JM, Deudero JJ, Chancey JH, Enikolopov G, Overstreet-Wadiche LS, Tsirka SE, Maticic-Savatic M, 2010. Microglia shape adult hippocampal neurogenesis through apoptosis-coupled phagocytosis. *Cell Stem Cell* 7 (4), 483–495. 10.1016/j.stem.2010.08.014. [PubMed: 20887954]
- Spangenberg EE, Lee RJ, Najafi AR, Rice RA, Elmore MR, Blurton-Jones M, West BL, Green KN, 2016. Eliminating microglia in Alzheimer's mice prevents neuronal loss without modulating amyloid- $\beta$  pathology. *Brain* 139 (Pt 4), 1265–1281. 10.1093/brain/aww016. [PubMed: 26921617]
- Tremblay ME, Lowery RL, Majewska AK, 2010. Microglial interactions with synapses are modulated by visual experience. *PLoS Biol.* 8 (11), e1000527. 10.1371/journal.pbio.1000527. [PubMed: 21072242]
- Ulrich JD, Finn MB, Wang Y, Shen A, Mahan TE, Jiang H, Stewart FR, Piccio L, Colonna M, Holtzman DM, 2014. Altered microglial response to A $\beta$  plaques in APPS1–21 mice heterozygous for TREM2. *Mol. Neurodegener* 9, 20. 10.1186/1750-1326-9-20. [PubMed: 24893973]
- Van Eldik LJ, Carrillo MC, Cole PE, Feuerbach D, Greenberg BD, Hendrix JA, Kennedy M, Kozauer N, Margolin RA, Molinuevo JL, Mueller R, Ransohoff RM, Wilcock DM, Bain L, Bales K, 2016. The roles of inflammation and immune mechanisms in Alzheimer's disease. *Alzheimers Dement (NY)* 2 (2), 99–109. 10.1016/j.trci.2016.05.001.
- Wang Y, Cella M, Mallinson K, Ulrich JD, Young KL, Robinette ML, Gilfillan S, Krishnan GM, Sudhakar S, Zinselmeyer BH, Holtzman DM, Cirrito JR, Colonna M, 2015. TREM2 lipid sensing sustains the microglial response in an Alzheimer's disease model. *Cell* 160 (6), 1061–1071. 10.1016/j.cell.2015.01.049. [PubMed: 25728668]
- Wang Y, Ulland TK, Ulrich JD, Song W, Tzaferis JA, Hole JT, Yuan P, Mahan TE, Shi Y, Gilfillan S, Cella M, Grutzendler J, DeMattos RB, Cirrito JR, Holtzman DM, Colonna M, 2016. TREM2-mediated early microglial response limits diffusion and toxicity of amyloid plaques. *J. Exp. Med* 213 (5), 667–675. 10.1084/jem.20151948. [PubMed: 27091843]
- Weinhard L, di Bartolomei G, Bolasco G, Machado P, Schieber NL, Neniskyte U, Exiga M, Vadisiute A, Raggioli A, Schertel A, Schwab Y, Gross CT, 2018. Microglia remodel synapses by presynaptic trogocytosis and spine head filopodia induction. *Nat. Commun* 9 (1), 1228. 10.1038/s41467-018-03566-5. [PubMed: 29581545]
- Welikovitch LA, Do Carmo S, Maglóczy Z, Malcolm JC, Le J, Klein WL, Freund T, Cuelllo AC, 2020. Early intraneuronal amyloid triggers neuron-derived inflammatory signaling in APP transgenic rats and human brain. *Proc. Natl. Acad. Sci. U. S. A* 117 (12), 6844–6854. 10.1073/pnas.1914593117. [PubMed: 32144141]
- Wilson EN, Do Carmo S, Iulita MF, Hall H, Austin GL, Jia DT, Malcolm JC, Foret MK, Marks AR, Butterfield DA, Cuelllo AC, 2018. Microdose Lithium NP03 diminishes pre-plaque oxidative

- damage and neuroinflammation in a rat model of Alzheimer's-like amyloidosis. *Curr. Alzheimer Res* 15 (13), 1220–1230. 10.2174/1567205015666180904154446. [PubMed: 30182855]
- Youmans KL, Tai LM, Kanekiyo T, Blaine Stine W Jr, Michon S-C, Nwabuisi-Heath E, Manelli AM, Fu Y, Riordan S, Eimer WA, Binder L, Bu G, Yu C, Hartley DM, LaDu MJ, 2012. Intraneuronal A $\beta$  detection in 5xFAD mice by a new A $\beta$ -specific antibody. *Mol. Neurodegener* 7 (8). 10.1186/1750-1326-7-8.
- Yuan P, Condello C, Keene CD, Wang Y, Bird TD, Paul SM, Luo W, Colonna M, Baddeley D, Grutzendler J, 2016. TREM2 haplodeficiency in mice and humans impairs the microglia barrier function leading to decreased amyloid compaction and severe axonal dystrophy. *Neuron* 90 (4), 724–739. 10.1016/j.neuron.2016.05.003. [PubMed: 27196974]
- Zhao Y, Wu X, Li X, Jiang LL, Gui X, Liu Y, Sun Y, Zhu B, Pina-Crespo JC, Zhang M, Zhang N, Chen X, Bu G, An Z, Huang TY, Xu H, 2018. TREM2 is a receptor for  $\beta$ -amyloid that mediates microglial function. *Neuron* 97 (5), 1023–1031. 10.1016/j.neuron.2018.01.031. [PubMed: 29518356]

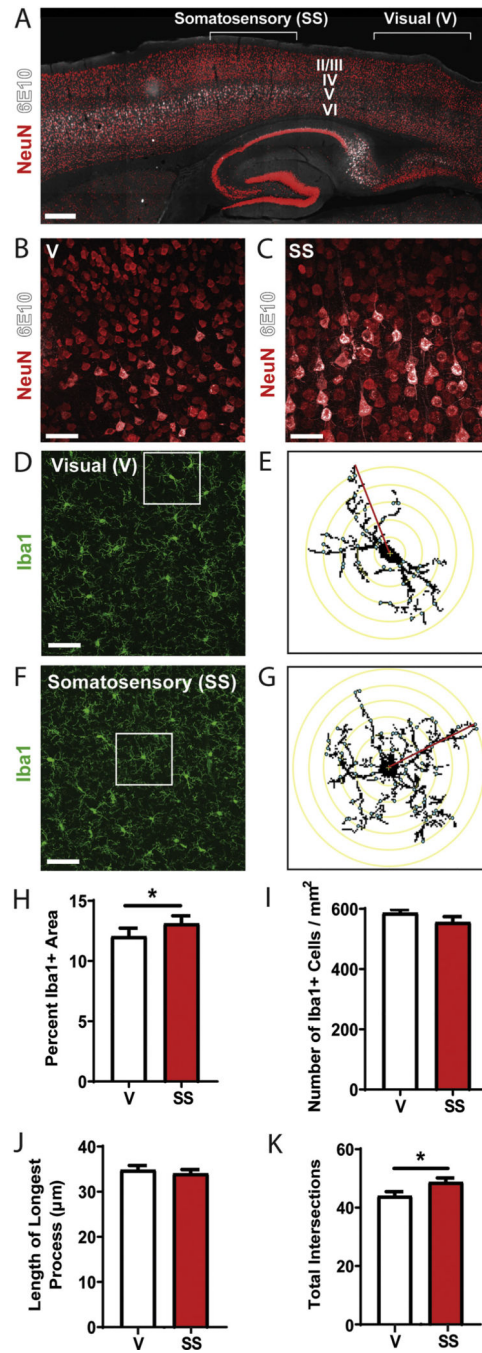


**Fig. 1.** Early amyloid accumulation drives changes in microglial coverage and morphology. (A) In 1-month-old 5XFAD mice, cortical layer V exhibits (B) low 6E10+ immunoreactivity in the visual cortex and (C) high 6E10+ signal in the somatosensory cortex. Microglia coverage, number, and morphology was evaluated in the (D, E) visual and (F, G) somatosensory cortices. Microglia coverage and cell number were determined by the averages of two images of the visual cortex and four images of the somatosensory cortex, respectively, per animal for 8 animals, and statistics and graphs represent the averages across all animals

per brain region. For Sholl analysis on microglia, 5–7 cells were analyzed across two ROIs in each brain region for 8 animals and analyses were performed on cellular replicates. Morphological measures assessed on individual microglia are shown in E and G: the distance from the center of the cell body to the edge of the longest process is shown in red, and the number of intersections between the cellular processes and each radius is shown in cyan. (H) Percent Iba1 area was increased in the higher amyloid region of the somatosensory cortex (SS) compared to the low amyloid laden visual (V) cortex using a paired *t*-test on  $n = 8$  biological replicates ( $V = 12.06 \pm 0.677$ ,  $n = 8$  mice;  $SS = 13.12 \pm 0.639$ ,  $n = 8$  mice; paired *t*-test  $p = 0.022$ ). (I) The number of microglia was not significantly different between these two brain regions ( $V = 587.0 \pm 10.48$ ,  $n = 8$  mice;  $SS = 556.4 \pm 17.89$ ,  $n = 8$  mice; paired *t*-test  $p = 0.118$ ). (J) An unpaired *t*-test revealed no significant differences between brain regions in the measured length of the longest process ( $V = 34.86 \pm 0.947$ ,  $n = 77$  cells;  $SS = 34.03 \pm 0.899$ ,  $n = 91$  cells; unpaired *t*-test  $p = 0.527$ ). (K) The total number of intersections were significantly increased in the somatosensory cortex (SS) relative to the visual cortex (V) ( $V = 44.03 \pm 1.43$ ,  $n = 77$  cells;  $SS = 48.77 \pm 1.41$ ,  $n = 103$  cells; unpaired *t*-test  $p = 0.020$ ). Scalebars for images A is 400  $\mu\text{m}$ , and B, C, D, and F are 50  $\mu\text{m}$ . Data are reported as mean  $\pm$  SEM. (For interpretation of the references to colour in this figure legend, the reader is referred to the web version of this article.)

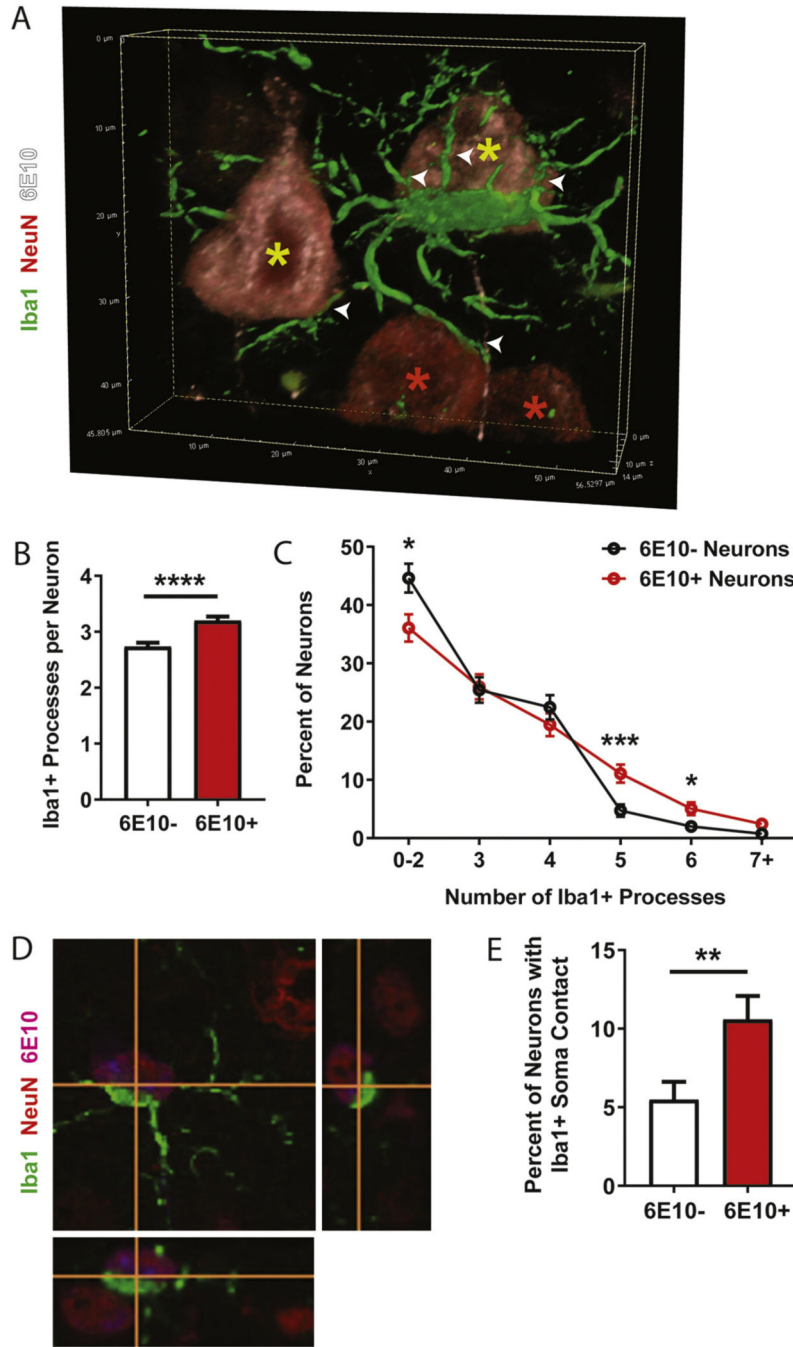


**Fig. 2.** Microglia show preferential engagement of amyloid laden neurons in pre-plaque animals. (A) A 3D-plane image showing an Iba1+ microglia making contact (white arrow heads) with its processes to 6E10+ (yellow asterisks) and 6E10- (red asterisks) neuronal cell bodies. (B) There is a significant increase in the number of Iba1+ microglial processes contacting 6E10+ neuronal cell bodies compared to neighboring 6E10- neuronal cell bodies in the somatosensory cortex (6E10- = 2.74 ± 0.068, *n* = 401 cells; 6E10+ = 3.20 ± 0.075, *n* = 416 cells; unpaired *t*-test *p* = 0.0001). (C) A similar distribution for the percent of neurons with

different degrees of microglial contact exists across 6E10<sup>-</sup> and 6E10<sup>+</sup> neuronal populations. However, minimal microglial engagement (0–2 processes) occurs for significantly more 6E10<sup>-</sup> neurons than 6E10<sup>+</sup> neurons, while high microglial engagement (5 or 6 processes) happens for a greater number of 6E10<sup>+</sup> neurons compared to 6E10<sup>-</sup> neurons (0–2 Processes (6E10<sup>-</sup> =  $44.64 \pm 2.486$ , n = 401 cells; 6E10<sup>+</sup> =  $36.06 \pm 2.36$ , n = 416 cells; unpaired t-test  $p = 0.0124$ ), 3 Processes (6E10<sup>-</sup> =  $25.44 \pm 2.18$ , n = 401 cells; 6E10<sup>+</sup> =  $25.96 \pm 2.15$ , n = 416 cells; unpaired t-test  $p = 0.864$ ), 4 Processes (6E10<sup>-</sup> =  $22.44 \pm 2.09$ , n = 401 cells; 6E10<sup>+</sup> =  $19.47 \pm 1.94$ , n = 416 cells; unpaired t-test  $p = 0.2969$ ), 5 Processes (6E10<sup>-</sup> =  $4.74 \pm 1.06$ , n = 401 cells; 6E10<sup>+</sup> =  $11.06 \pm 1.54$ , n = 416 cells; unpaired t-test  $p = 0.0008$ ), 6 Processes (6E10<sup>-</sup> =  $2.00 \pm 0.699$ , n = 401 cells; 6E10<sup>+</sup> =  $5.05 \pm 1.08$ , n = 416 cells; unpaired t-test  $p = 0.0184$ ), 7 Processes: 6E10<sup>-</sup> =  $0.748 \pm 0.431$ , n = 401 cells; 6E10<sup>+</sup> =  $2.40 \pm 0.752$ , n = 416 cells; unpaired t-test  $p = 0.0587$ )). (D) Iba1<sup>+</sup> microglia can make soma-soma contacts with NeuN<sup>+</sup> neurons as shown in three different image planes. (E) The percent of neuronal cell bodies with Iba1<sup>+</sup> cell soma contact is higher for 6E10<sup>+</sup> neurons compared to neighboring 6E10<sup>-</sup> neurons (6E10<sup>-</sup> =  $5.49 \pm 1.14$ , n = 401 cells; 6E10<sup>+</sup> =  $10.58 \pm 1.51$ , n = 416 cells; unpaired t-test  $p = 0.0075$ ). Analyses were performed on 401 6E10<sup>-</sup> cells and 416 6E10<sup>+</sup> cells over two ROIs in the somatosensory cortex across 8 animals and statistics were performed on cellular replicates using unpaired *t*-tests. Data are reported as mean  $\pm$  SEM. (For interpretation of the references to colour in this figure legend, the reader is referred to the web version of this article.)

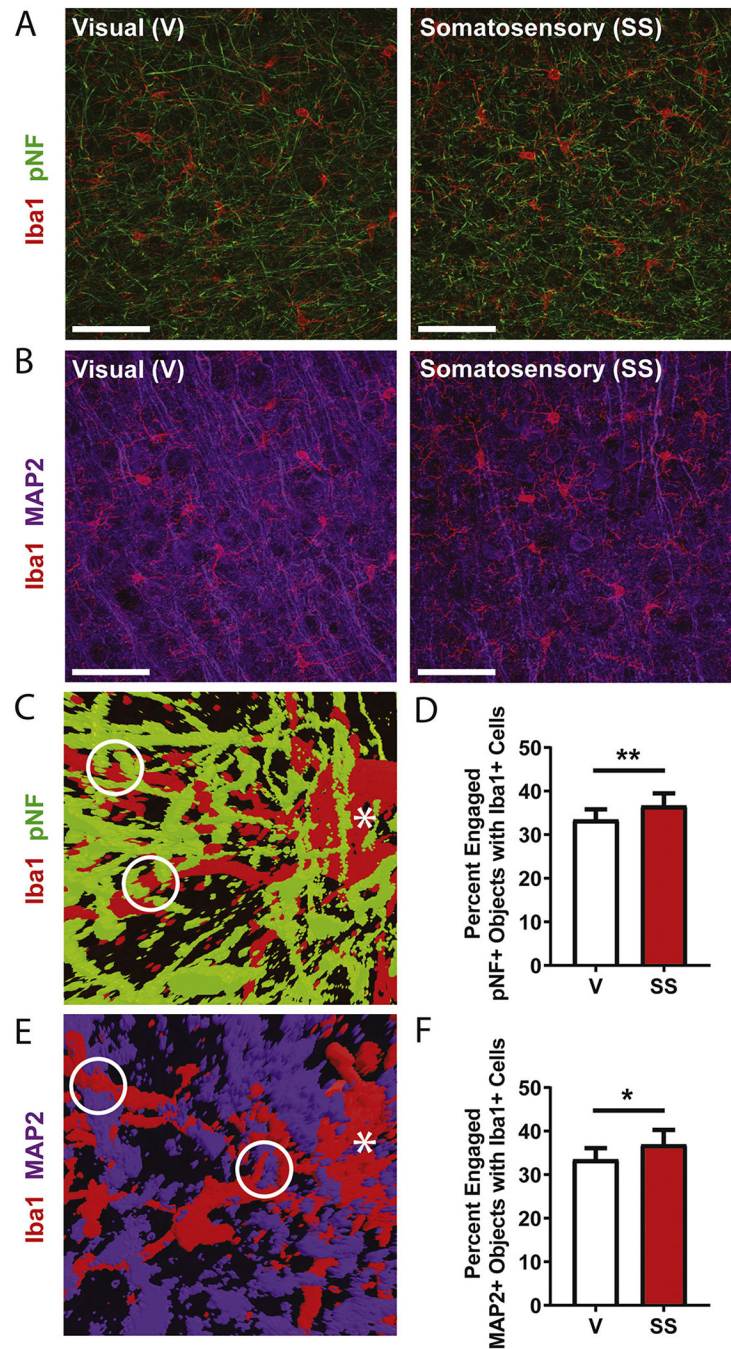


**Fig. 3.** Amyloid accumulation promotes enhanced microglia-neurite interactions. (A) Representative unprocessed images of Iba1+ microglia and the axonal marker phosphorylated neurofilament (pNF) and (B) Iba1+ microglia and the dendritic marker MAP2 taken from layer V of the somatosensory and visual cortices. (C) Images were thresholded and example binary 3D representations of the images in A are shown. Examples of Iba1+ microglial processes (cell bodies labeled\*) within  $2 \mu\text{m}^3$  of neurites are indicated by white circles. (D) The number of processes within this distance was analyzed for pNF-

positive axons, and normalized to the total pNF signal in each field. This was significantly elevated in the amyloid-enriched somatosensory cortex ( $V = 33.42 \pm 2.41$ ,  $n = 8$  mice;  $SS = 36.66 \pm 2.83$ ,  $n = 8$  mice; paired t-test  $p = 0.0059$ ). Similarly, microglial processes also contact (E) MAP2-positive dendrites, shown here as 3D representations of thresholded images from B. (F) This type of microglial-neurite contact is also increased in the presence of high amyloid levels in the somatosensory cortex compared to the visual cortex ( $V = 33.48 \pm 2.64$ ,  $n = 8$  mice;  $SS = 36.91 \pm 3.34$ ,  $n = 8$  mice; paired t-test  $p = 0.0415$ ). Paired t-tests were performed between brain regions where an average was taken of two ROIs per cortical region for each animal ( $n = 8$ ). Scalebars for images A and B are  $50 \mu\text{m}$ . Data are reported as mean  $\pm$  SEM.

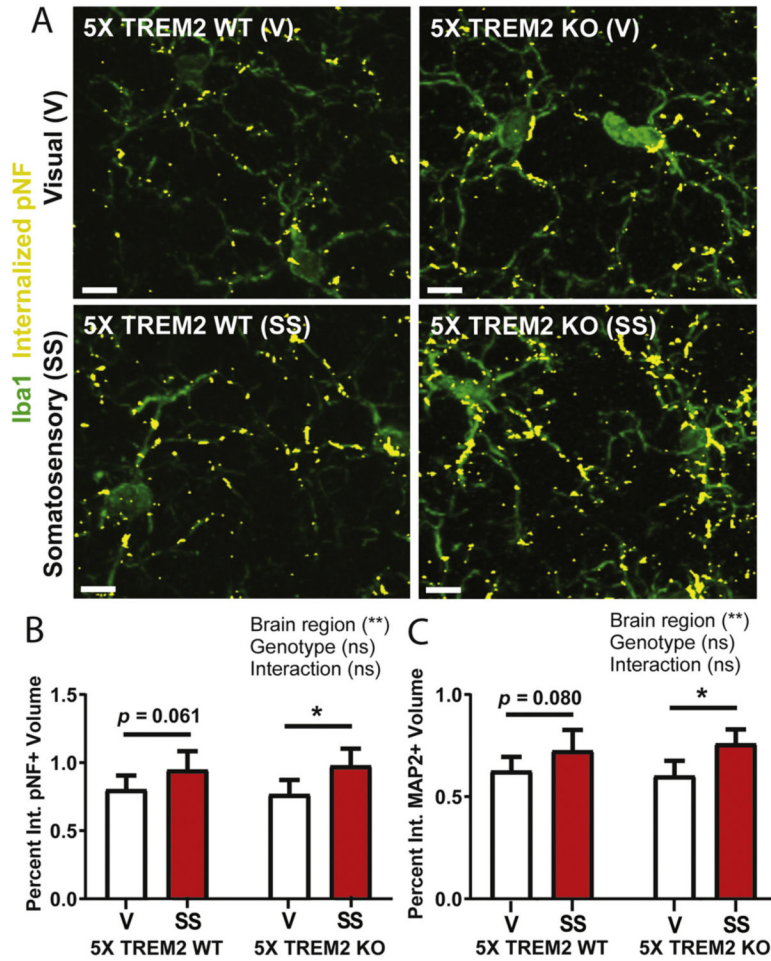


**Fig. 4.** Increased microglial uptake of neurites occurs in high amyloid areas and does not require the phagocytic receptor TREM2. (A) Representative images are shown of Iba1+ microglia with internalized pNF+ axons in the somatosensory and visual cortices of 5x FAD (or 5x) TREM2 WT and 5x TREM2 KO mice. Quantification of internalized (B) pNF+ axons and (C) MAP2+ dendrites in microglia with statistical analysis by 2-way ANOVA reveals a significant effect of brain region on internalized neurites. B: (WT(V) = 0.802 ± 0.104, n = 8 mice; WT(SS) = 0.947 ± 0.137, n = 8 mice; KO (V) = 0.767 ± 0.105, n = 6 mice; KO(SS) = 0.977 ± 0.126, n = 6 mice; 2-way ANOVA: Brain region  $p = 0.0021$ , Genotype  $p = 0.990$ , Interaction  $p = 0.494$ ; Bonferroni post-hoc test,  $p$  values corrected for multiple comparisons: 5x TREM2 WT  $p = 0.0610$ , 5x TREM2 KO  $p = 0.0199$ ), C: (WT(V) = 0.626 ± 0.068, n = 8 mice; WT(SS) = 0.725 ± 0.101, n = 8 mice; KO(V) = 0.602 ± 0.074, n = 6 mice; KO(SS) = 0.759 ± 0.0702, n = 6 mice; 2-way ANOVA: Brain region  $p = 0.0021$ , Genotype  $p = 0.966$ , Interaction  $p = 0.391$ ; Bonferroni post-hoc test,  $p$  values corrected for multiple comparisons: 5x TREM2 WT  $p = 0.0801$ , 5x TREM2 KO  $p = 0.0161$ ). There was no significant effect of genotype or interaction. Bonferroni post-hoc tests revealed significant increases in neurite uptake in the somatosensory cortex within 5x TREM2 KO mice. Analyses were performed on an average taken from two ROIs per cortical region for each animal (n = 8 5x TREM2

WT; n = 6 5× TREM2 KO). Scalebars for images are 20 μm. Data are reported as mean ± SEM.

Author Manuscript

Author Manuscript

Author Manuscript

Author Manuscript